Mech. Adv. Technol., Vol. 8, No. 3, 2024, pp. 280–288

DOI: 10.20535/2521-1943.2024.8.3(102).304079

UDK 622.24

Simulation of the effect of multi-particle temperature on Al6061 coating porosity based on Coupled Eulerian-Lagrangian(CEL) method

Tan Kun[1]

Received: 15 May 2024 / Revised: 26 June 2024 / Accepted: 7 September 2024

Abstract. *Cold spray is a solid-state deposition technology widely used in additive manufacturing. The particles temperature is mostly used to adjust the porosity of the coating. This article uses Pyhon script to model the multi-particle model; then the multi-particle model is nested in the CEL deposition model to simulate the actual cold spray multi-particle deposition process; The CEL method has the characteristics of high accuracy and robustness and was selected as the simulation method for the multi-particle deposition model. The porosity of the coating is expressed by studying the value of the EVF void area in the Euler domain. Multiple groups of samples were taken on the coating surface to calculate the porosity of each group, and the average value was finally taken as the porosity of the entire coating. Numerical results show that increasing the particle temperature can effectively reduce the porosity of the coating. The average porosity of the coating under the particles temperature conditions are 600 K: 5.08 %; 650 K: 4.02 %; 700 K: 3.58 %; deposition completed the inside of the coating appears to be compacted. The substrate temperature will affect the combination of the coating and the substrate. It is recommended that the temperature difference between the particles and the substrate should not be too large. The CEL method simulates the process of cold spray multi-particle deposition, which is an effective method to observe and predict the porosity of the coating, which is also unachievable by the SPH and ALE methods.*

Keywords: *cold spraying, CEL, deposition, temperature, multi-particle, porosity, substrate.*

1. Introduction

Cold Spray (CS) is a solid-state deposition technology [1] widely used in additive manufacturing. Pressurized gas in the nozzle accelerates particles (5–50 um) to high speeds (300–1200 m/s), and the particles impact the substrate at high speed. A dense and high-quality coating is formed under the action of deformation [2]–[5]. Adiabatic shear instability and local plastic flow are considered to be the main mechanisms of particle/substrate and particle/particle bonding [6], [7]. The formation of the coating can be seen as an iterative process, with repeated impact-deformation-adhesion between particles. In the cold spray process, porosity is an important indicator. Porosity that is not easily controlled will cause the structure to be brittle, thus affecting the mechanical properties of the coating [8], [9]. Factors affecting the porosity level can be divided into technical parameters (Gas temperature and pressure; Particles velocity, temperature, size and shape; substrate temperature; spraying distance and angle) and structural parameters (parameters of Laval nozzle) [10]–[17].

In cold spraying, particle/substrate, particle/particle contact occurs within tens of nanoseconds and follows highly transient nonlinear and dynamic rules [7], [18], [19]; Interactions during deposition are difficult to analyze experimentally, so numerical simulations are useful in helping to understand particle/substrate and particle/particle bonding mechanisms. The simulation methods currently used include: Pure Lagrangian [20]–[23], Arbitrary Lagrangian Euler (ALE) [24]–[26], SPH (Smoothed Particle Hydrodynamics) [27], [28], Pure Eulerian [29] and Coupled Eulerian Lagrangian (CEL) [30]; The ALE numerical method combines the characteristics of pure Lagrangian analysis and pure Eulerian analysis, and is often used to simulate solids and fluids [7], [11], [31]–[34]. It is not the best choice when spray particles experience excessive deformation. [35]; Wang used the ALE method to simulate the deposition on Cu particles/cast iron substrate and the deposition on stainless steel particles/Q235 steel substrate,

✉ *Tan Kun*
tankun09@126.com

[1] *National aerospace university "Kharkiv Aviation Institute", Kharkiv, Ukraine*

and studied the temperature, plastic deformation and bonding morphology of the particles [36]; Wang used the ALE method to simulate the distribution of residual stress after deposition of NiCrAl/TA-15 titanium alloy substrate [37]. SPH is a meshless adaptive Lagrangian calculation method for continuous dynamics problems. It is very useful for simulating high-speed impact problems [38], [39]. Yin uses the SPH method to simulate the deposition of powders with different sizes. The relationship between the effective plastic strain in the process [39]. The CEL method has been proven to be more suitable for analyzing large deformation problems that occur during cold spraying. The method has higher accuracy and robustness than other finite element techniques in the range of large deformation, large displacement and large strain. Its advantage is that particles are wrapped in Eulerian domains, which avoids the need for remeshing and highly distorted elements [18]; CEL cannot numerically study the deformation of particles. Instead, it tracks the material as it flows through the grid by calculating the Eulerian volume fraction in each cell. If the material completely fills the cell, its volume fraction is 1, which is not present in the element. For this material, its volume fraction is 0, and the sum of the volume fractions of all materials in the unit is less than 1, then the rest of the unit will automatically fill the void material, and the void material has no mass and strength [40]. Xie analysis concluded that the CEL method is the best way to study substrate deformation and predict sample porosity levels [18]. Many scholars have studied the large deformation of particles during cold spraying through the CEL method [7], [25], [41]–[43]; M [44] used the CEL method to study the thermal softening effect of single particle temperature. As the particle temperature increases, the particle flatness rate increases; thus further studying porosity. S [45] studied the impact of single Cu particles on Al substrate, and increasing the particle temperature and speed can increase the density of sprayed samples; The above are dedicated to predicting the porosity level of fabricated samples.

There are currently two methods for checking the porosity of coatings. One is to obtain experimentally and characterize the coating through cross-sectional Scanning electron microscopy (SEM) image analysis [21], [48] or X-ray microtomography (XMT) [49]; The other is to use numerical simulation methods to predict the porosity of the coating [45], [46], [50]–[52]. The single-particle deposition model simulated by the CEL method cannot represent the interaction between coating accumulation, particle size, velocity and temperature [53]. Therefore, it is necessary to simulate the process of multi-particle formation of coatings. The multi-particle deposition model is between the microscopic method of single particle simulation and the macroscopic method of homogeneous material deposition [46]; Multi-particle deposition models can be used to simulate complex interactions between multiple particles, which cannot be achieved by single-particle deposition models. Matteo [45] used the CEL method to simulate the spraying of multi-particle Ti-Al and Ti-Cu particles. The weight of the particles and the mass of the raw material particles were calculated to calculate the corresponding volume percentage, thereby predicting the porosity of the coating. This is not a direct study of the porosity of the coating after deposition. Weiller [46] used the CEL method to simulate the deposition of multi-particle Al/Al2017 to study the formation mechanism of porosity. They concluded that interface porosity and stacking porosity have a great influence on the porosity of the coating. The interface porosity is determined by the particles. Caused by the arrangement between them, stacking porosity is caused by changes in particle density in gas flow; randomly generated particles will cause irrationality in the distribution of particles in the Euler domain, thus affecting the final porosity result.

This study simulates the deposition of Al6061 particles/substrate by establishing a multi-particle deposition model and changes the particle temperature to study the porosity of the coating. The multi-particle model is implemented through Python programming code, embedded in the CEL deposition model, and the porosity of the Al6061 coating is predicted. The advantage of using Python code to establish a multi-particle model is that the multi-particles are arranged irregularly in a specified space, which can more accurately characterize the characteristics of real cold spray particles. The CEL method has the characteristics of high accuracy and robustness and was selected as the simulation method for the multi-particle deposition model. Multiple groups of sampling methods are used in the coating to calculate the porosity of the sampling groups to further characterize the entire porosity. Take several groups of cuboid samples from the coating, and calculate the value of the void area of each group of samples. Finally, find the average value as the value of the void area of the coating under a certain working condition, and identify this value as the porosity of the coating. This is a new method to predict the porosity of cold spray coatings through numerical simulation

2. Multi-particle deposition model

The CS process can be viewed as a process in which multiple particles continuously impact the substrate. Several different finite element techniques described in the introduction are used to model the spatial discretization of CS processes. The CEL method is considered to be the most robust and accurate solution for simulating the CS process at present. Its characteristic is that the CEL deposition model contains both the Eulerian domain and the Lagrangian domain; In the Eulerian domain, granular materials are not constrained by predefined elemental discretizations; Particles flow freely within a discrete domain of fixed elements, and the volume fraction value characterizes the specific number of particles that each element can contain at any given time and is compatible with large deformations of particles in depositions.

2.1. Multi-Particle Model and Material Model

The particle size distribution of multi-particles is shown in Fig. 1. The cumulative probability distribution of particle size is described by the log-normal function. Choose a multi-particle particle size of 30–50 um and particles number of 200. The establishment of the multi-particle model is implemented using Python scripts. The multi-particle model is established through a custom algorithm. By inputting the number and volume percentage of particles, multiple particles are randomly distributed in the Euler domain. In this process, overlap between particles is avoided. Its principle: whether the distance between particles in spatial coordinates is greater than the sum of the radii between particles, a mathematical expression to avoid particle overlap.

$$\sqrt{\left(x_i - x_j\right)^2 + \left(y_i - y_j\right)^2 + \left(z_i - z_j\right)^2} > R_1 + R_2, \quad (1)$$

where $\left(x_{i/j}, y_{i/j}, z_{i/j}\right)$ is the spatial coordinate of the particle in the Euler domain. R_1 and R_2 are the radius of the particles.

The cold spray process involves high strain rates, plastic deformation and temperature changes; In order to simulate the deposition effect of Al6061 particles on the same substrate, it is assumed that the material is isotropic; The bilinear Johnson-Cook (J-C) plasticity model is added to characterize the high dependence of rate and temperature. Formulas 2 and 3 are the definitions of the J-C model; At the same time, the erosion and cracking phenomena that occur under high-speed impact must also be considered, and the Failure initiation model must be added. All model parameters are shown in Table 1 [54], [56]. The ratio of plastic energy converted into heat is 0.9 [55].

$$\sigma = \left(A + B\varepsilon_p^n\right)\left[1 + C\ln\left(\frac{\dot{\varepsilon}_p}{\dot{\varepsilon}_0}\right)\right]\left[1 - \left(\frac{T - T_r}{T_m - T_r}\right)^m\right]; \quad (2)$$

$$C = \begin{cases} C_1 \quad and \quad \dot{\varepsilon}_0 = 1 \quad if \quad \dot{\varepsilon}_p \le \dot{\varepsilon}_c \\ C_2 \quad and \quad \dot{\varepsilon}_0 = \dot{\varepsilon}_c \quad if \quad \dot{\varepsilon}_p > \dot{\varepsilon}_c \end{cases}. \quad (3)$$

where σ is the flow stress, $\dot{\varepsilon}_p$ is the strain rate, $\dot{\varepsilon}_0$ is the reference strain rate, T_r is a reference temperature, T_m is the melting temperature of the material, A, B, n and m are the model parameters, C_1 and C_2 are coefficients that describe the additional increase in flow stress when the applied $\dot{\varepsilon}_p$ is greater than the critical plastic strain rate [57].

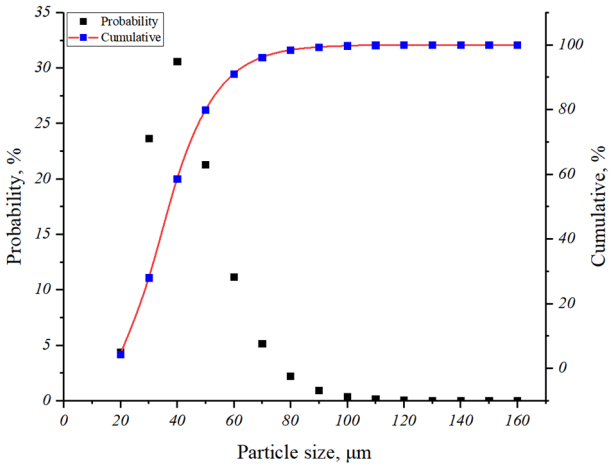

Fig. 1. Particle size distribution and cumulative distributions

2.2. Deposition model

The work of this article is to study the effect of particles at different temperatures on the porosity of the coating. All Al6061 particles are given a velocity value of 585 m/s, so that all particles can deposit; The temperature of the particles is 600 K–700 K, increasing by 50 K for each working condition; the substrate temperature is 400 K; Assign a coupled temperature-displacement dynamic step with an

Table 1. Material properties for Al6061

Properties	Parameters	Value
General	Density ρ, (kg/m^3)	2700
	Specific heat Cp, J/(kg·K)	1009
	Thermal conductivity coefficient λ, W/(m·K)	155
	Melting temperature Tm, (K)	925
	Inelastic heat fraction	0.9
	Elastic modulus, (Gpa)	69.11
	Poisson's ratio, ν	0.331
	Shear modulus, (Gpa)	25.9
Johnson-Cook plasticity parameters	*A* (Mpa), *B* (Mpa), *n*, *m*	270, 154.3, 0.239, 1.42
	Reference strain rate	1
	Reference temperature Tref, (K)	298
	C_1, C_2, $\dot{\varepsilon}_c$	0.002, 0.0029, 597.2
Failure initiation	d_1, d_2, d_3, d_4, d_5	– 0.56, 1.45, 0.47, 0.011, 1.6

appropriate time period to track the entire multi-particle impact process from the start of the simulation to the complete stop of all particles, with a total range of 970 to 1000 ns. As mentioned above, all particles are included in the Euler domain, so the entire process of simulating multi-particle deposition by the deposition model will be completed in the Euler domain. The model of the base material is Lagrangian, so part of the Euler domain in the entire deposition model should be nested in the base material to ensure that the coating formed after the deposition is still in the Euler domain, ensuring the integrity of the calculation results; It should be noted that the partial mesh size of the Euler domain and the deposition substrate should be kept consistent as much as possible; Fig. 2 shows 1/4 section view of multi-particle deposition model. The contact algorithm automatically calculates and tracks the interface between the two domains, ignoring the heat exchange between the particles and the substrate, considering the process to be adiabatic [7].

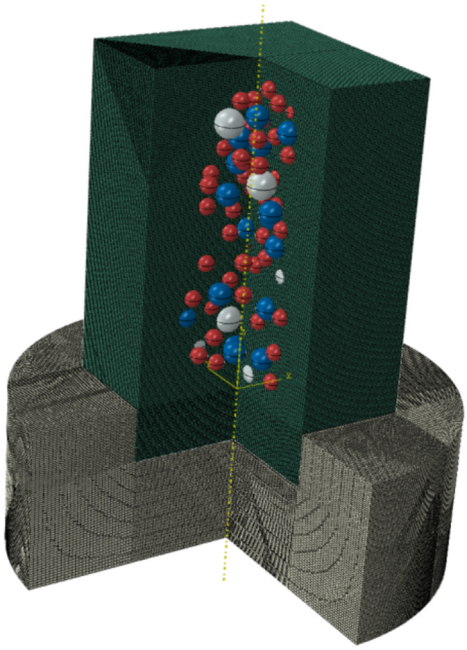

Fig. 2. 1/4 section view of multi-particle deposition model

3. Results and Discussion

Fig. 3 shows a cross-sectional view of the Euler volume fraction(EVF) of voids in the coating formed after multi-particle depositions at different temperatures. The red EVF void value is 1, indicating the gap area, the blue EVF void value is 0, indicating that the element is filled with material; Observing the value of EVF void can characterize the porosity of the coating. It can be found from the fig. 4 that there are void areas inside the coating; the thickness of the coating decreases significantly when the temperature of the particles is increased, indicating that increasing the temperature of the particles is beneficial to the CS process. Observing the cross-section, the void value inside the coating decreases. Therefore, the porosity of the coating can be characterized by calculating the value of the void area of the coating after simulated spraying, which is what the Lagrangian method cannot achieve; this is due to the fact that the grid in the Eulerian domain in the CEL method does not follow the the particles change due to deformation. In order to better and more accurately express the porosity of the coating, we take several groups of cuboid samples in the coating, calculate the value of the void area of each group of samples, and finally obtain the average value as the coating's porosity under certain working conditions. The value of the void area is considered to be the porosity of the coating.

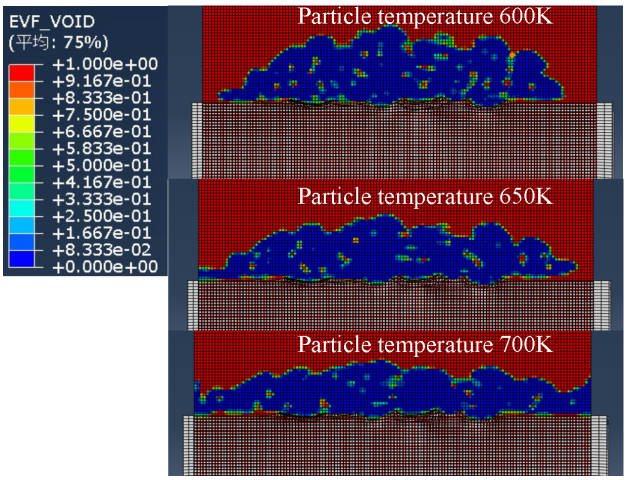

Fig. 3. Cross-sectional view of Euler volume fraction voids of a multi-particle coating

Fig. 4 shows the mutual conversion between kinetic energy and internal energy of particles in the entire deposition model. Almost all kinetic energy is converted into internal energy, and the process is stable, indicating that the entire deposition model has good stability.

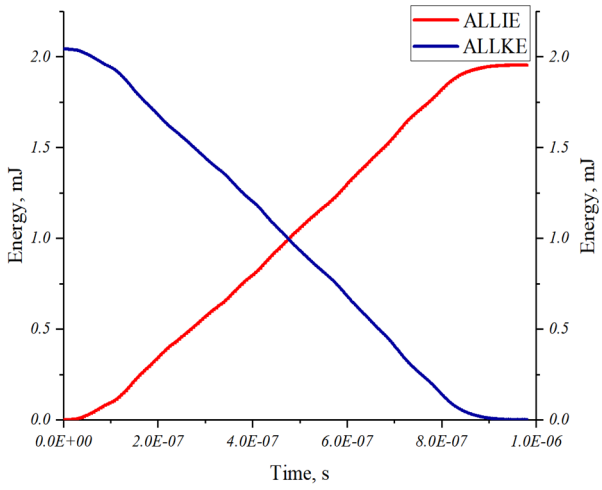

Fig. 4. ALLKE and ALLIE variation for the whole model during the entire simulation

Four groups of Euler volume fraction cuboids with dimensions of 900 um × 900 um × 30 um were selected from the coating for each working condition, and the cuboid samples were distributed as far as possible inside the center of the coating, as shown in the sampling area map in Fig. 5. In the Python script, most of the multi-particle arrangements tend to be in the central area; the coating at the same height is selected for sampling under all working con-

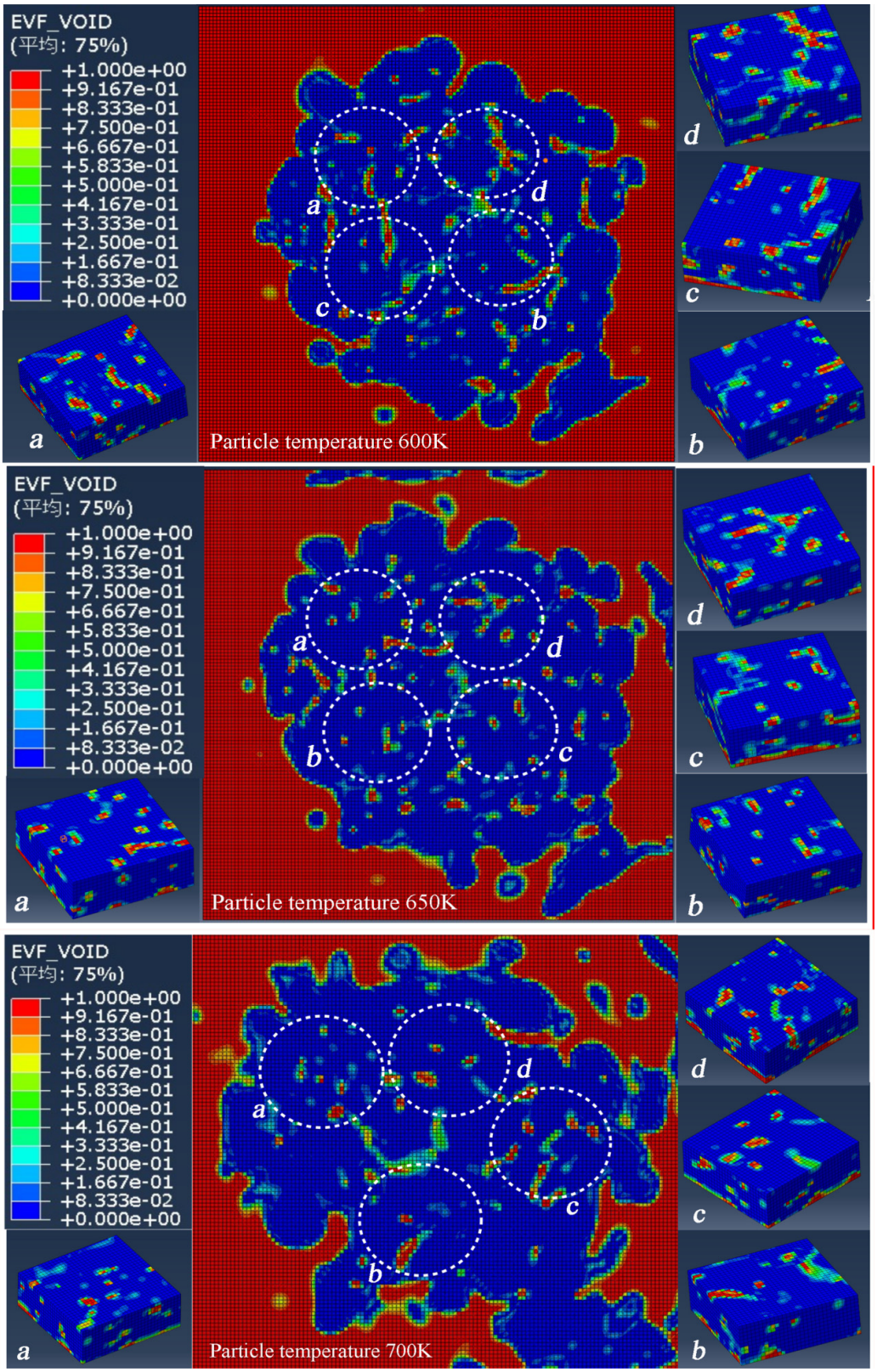

Fig. 5. Sampling area map

ditions, and then 4 groups of samples are selected from this layer, which allows the final calculation results to characterize the coating The porosity is more representative. It can be seen from observation that when the coating height is 90 um, increasing the temperature of the particles will reduce the void value of the coating with the same height, which is the same as the result expressed in Fig. 3; Increasing the particles temperature can reduce the porosity, which is consistent with our conjecture. Fig. 6 shows the average porosity of the coating obtained at different temperatures; It is obvious from Fig. 6 that increasing the temperature of the particles can reduce the porosity. When the particle temperature goes from 600 K to 650 K, the porosity of the coating decreases faster than when the particle temperature changes from 650 K to 700 K. This shows that continuously increasing the particle temperature is not the best way to reduce porosity. To ensure the lowest porosity, there is an optimal particle temperature range. The particle temperature is 600 K, the average porosity of the coating is: 5.08 %; The particle temperature is 650 K, the average porosity of the coating is: 4.02 %; The particle temperature is 700 K, the average porosity of the coating is: 3.58 %. This is the result obtained using single factor research method.

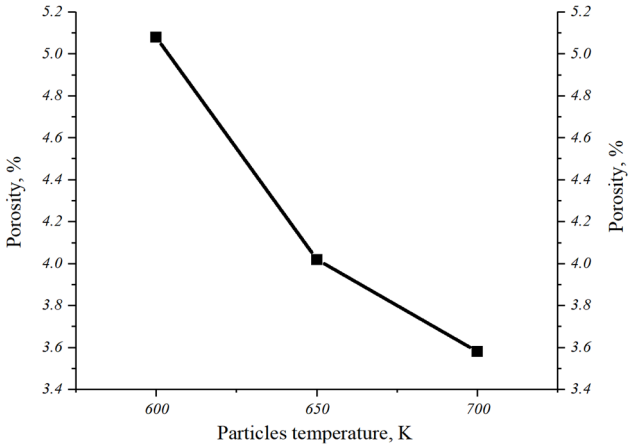

Fig. 6. Average porosity of the coating obtained at different temperatures

In order to understand the process of porosity reduction in more detail, the void area percentages of 12 groups of Euler volume fraction cuboids under temperatures conditions were compared individually, and then each group of Euler volume fraction cuboids was divided into 10 layers and calculated separately. Their value for the void area of the coating. As shown in Fig. 7 porosity of each layer in the sampling group are shown. The first set of data corresponds to the top of the coating, and the 10th set of data corresponds to the bottom of the coating; Combined with Fig. 6, It can be seen that the porosity curve decreases as the particle temperature increases, and the porosity of each layer corresponding to the same position of the coating also decreases. The porosity of the coating at the bottom layer is the highest, and the porosity of the coatings on layers 6–9 is lower. This happens to indicate that the inside of the deposited coating is compacted, which is consistent with the CS process. The reason for the greater porosity between the particles and the substrate is that the temperature difference between the two is large. Compared with the interfacial bonding between the particles, the temperature of the substrate has little effect on the porosity [50]. Increasing the substrate temperature will facilitate the connection between the particles and the substrate [14]. It is suggested here that appropriately raising the substrate temperature will benefit the CS process and meet the requirement that the temperature difference between the particles and the substrate should not be too large.

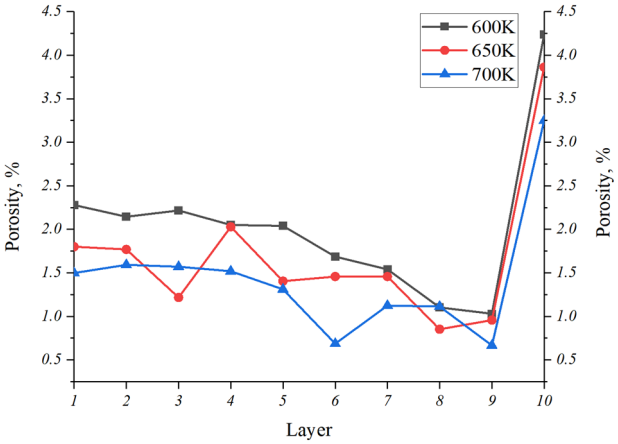

Fig. 7. Porosity of each layer in the sampling group

4. Conclusion

This article studies the relationship between particle temperature and coating porosity, and uses Python programming software to embed the multi-particle model in the multi-particle Al6061 deposition model established by the CEL method to predict the coating porosity.

The advantage of implementing the multi-particle model through Python programming software is that it can accurately characterize the disordered arrangement of multiple particles in Euler domain.

The results show that the average porosity of the coating under the three temperature conditions are 600 K: 5.08 %; 650 K: 4.02 %; 700 K: 3.58 %; Increasing the temperature of the particles can effectively reduce the porosity of the coating; during the deposition process of multiple particles, the inside of the deposited coating will be compacted. In the CEL method, the grid in the Euler domain will not deform with the particles, and the value of the EVF void area can accurately express the porosity of the coating. The substrate temperature will affect the combination of coating and particles with the substrate, It is recommended that the temperature difference between the particles and the substrate should not be too large. Finally it is recommended to study the multi-factor coupling affecting the porosity of the coating.

References

[1] K. Tan, "Analysis of spray particles entrance of Right-angle cold spray nozzle based on CFD", *Mech. Adv. Technol*., vol. 7, no. 3 (99), pp. 325–329, Dec. 2023, doi: 10.20535/2521-1943.2023.7.3.292244.

[2] K. Ogawa, K. Ito, K. Ichimura, Y. Ichikawa, S. Ohno and N. Onda, "Characterization of low-pressure cold-sprayed aluminum coatings", *Journal of Thermal Spray Technology*, 17, pp. 728–735, 2008, doi: 10.1007/s11666-008-9254-5.

[3] H. Takana, K. Ogawa, T. Shoji & H. Nishiyama, "Computational simulation of cold spray process assisted by electrostatic force", *Powder Technology*, 185(2), pp. 116‑123, 2008, doi: 10.1016/j.powtec.2007.10.005.

[4] S. Guetta, M. H. Berger, F. Borit et al., "Influence of particle velocity on adhesion of cold-sprayed splats", *Journal of thermal spray technology*, 18, pp. 331–342, 2009, doi: 10.1007/s11666-009-9327-0.

[5] Y. Ichikawa, K. Sakaguchi, K. Ogawa et al., "Deposition mechanisms of cold gas dynamic sprayed MCrAlY coatings", *Thermal Spray 2007: Global Coating Solutions*, 1212, pp. 14–16, 2007, doi: 10.31399/asm.cp.itsc2007p0054.

[6] M. Grujicic, C. L. Zhao, W. S. DeRosset & D. Helfritch, "Adiabatic shear instability based mechanism for particles/substrate bonding in the cold-gas dynamic-spray process", *Materials & design*, 25(8), pp. 681–688, 2004, doi: 10.1016/j.matdes.2004.03.008.

[7] H. Assadi, F. Gartner, T. Stoltenhoff, and H. Kreye, "Bonding Mechanism in Cold Gas Spraying", *Acta Mater.*, 51, pp. 4379‑4394, 2003, doi: 10.1016/S1359-6454(03)00274-X.

[8] E. Bakan, D. Marcano, D. Zhou et al., "$Yb_2Si_2O_7$ environmental barrier coatings deposited by various thermal spray techniques: a preliminary comparative study", *Journal of thermal spray technology*, Vol. 26, pp. 1011–1024, 2017, doi: 10.1007/s11666-017-0574-1.

[9] S. Weiller & F. Delloro, "A numerical study of pore formation mechanisms in aluminium cold spray coatings", *Additive Manufacturing*, Vol. 60, 103193, 2022, doi: 10.1016/j.addma.2022.103193.

[10] V. S. Shikalov, V. F. Kosarev, T. M. Vidyuk, S. V. Klinkov & I. S. Batraev, "Mechanical and tribological properties of cold sprayed composite Al-B_4C coatings", *In AIP Conference Proceedings*, Vol. 2448, No. 1, AIP Publishing, (2021, December), doi: 10.1063/5.0073401.

[11] A. Moridi, S. M. Hassani-Gangaraj & M. Guagliano, "A hybrid approach to determine critical and erosion velocities in the cold spray process", *Applied Surface Science*, Vol. 273, pp. 617–624, 2013, doi: 10.1016/j.apsusc.2013.02.089.

[12] K. Tan, S. Markovych, W. Hu, O. Shorinov & Y. Wang, "Review of application and research based on cold spray coating materials", *Aerospace Technic and Technology*, Vol. 1, pp. 47–59, 2021, doi: 10.32620/aktt.2021.1.05.

[13] W. Hu, S. Markovych, K. Tan, O. Shorinov & T. Cao, "Surface repair of aircraft titanium alloy parts by cold spraying technology", *Aerospace Technic and Technology*, No. 3, pp. 30–42, 2020, doi: 10.32620/aktt.2020.3.04.

[14] K. Tan, S. Markovych, W. Hu et al., "On the characteristics of cold spray technology and its application in aerospace industries", *In IOP Conference Series: Earth and Environmental Science*, Vol. 719, No. 3, p. 032023, 2021. IOP Publishing, doi: 10.1088/1755-1315/719/3/032023.

[15] W. Hu, K. Tan, S. Markovych, and T. Cao, "Research on structure and technological parameters of multi-channel cold spraying nozzle", *EEJET*, vol. 5, no. 1(113), pp. 6–14, Oct. 2021, doi: 10.15587/1729-4061.2021.242707.

[16] W. Hu, K. Tan, S. Markovych & T. Cao, "Structural optimization of the special cold spraying nozzle via response surface method", *In Conference on Integrated Computer Technologies in Mechanical Engineering‑Synergetic Engineering* Cham: Springer International Publishing, pp. 110–122, 2021, doi: 10.1007/978-3-030-94259-5_11.

[17] T. Kun, H. W. Jie, S. Markovych, Y. Wang, "Dimet laval nozzle expansion section analysis and optimization", *Journal of Engineering Sciences*, Vol. 8(2), pp. 6–10, 2021, doi: 10.21272/jes.2021.8(2).f2.

[18] J. Xie, D. Nélias, H. Walter-Le Berre et al., "Simulation of the cold spray particle deposition process", *Journal of Tribology*, Vol. 137(4), 041101, 2015, doi: 10.1115/1.4030257.

[19] S. Rahmati & A. Ghaei, The use of particle/substrate material models in simulation of cold-gas dynamic-spray process", *Journal of thermal spray technology*, Vol. 23, pp. 530–540, 2014, doi: 10.1007/s11666-013-0051-4.

[20] P.-E. Leger, Rôle de la microstructure sur les mécanismes de corrosion marine d'un dépôt à base d'aluminium élaboré par projection dynamique par gaz froid ("cold spray"), Ph.D. thesis, Mines Paristech, 2018. https://pastel.archives-ouvertes.fr/tel-03118364.

[21] T. Schmidt, F. Gärtner, H. Assadi, and H. Kreye, "Development of a Generalized Parameter Window for Cold Spray Deposition", *Acta Mater*., Vol. 54, pp. 729–742, 2006, doi: 10.1016/j.actamat.2005.10.005.

[22] K. Kim, W. Li & X. Guo, "Detection of oxygen at the interface and its effect on strain, stress, and temperature at the interface between cold sprayed aluminum and steel substrate", *Applied Surface Science*, Vol. 357, pp. 1720–1726, 2015, doi: 10.1016/j.apsusc.2015.10.022.

[23] V. Lemiale, P. C. King, M. Rudman et al., "Temperature and strain rate effects in cold spray investigated by smoothed particle hydrodynamics", *Surface and Coatings Technology*, Vol. 254, pp. 121–130, 2014, doi: 10.1016/j.surfcoat.2014.05.071.

[24] F. Delloro, M. Jeandin, D. Jeulin et al., "A morphological approach to the modeling of the cold spray process", *Journal of Thermal Spray Technology*, Vol. 26, pp. 1838‑1850, 2017, doi: 10.1007/s11666-017-0624-8.

[25] W. Y. Li & W. Gao, "Some aspects on 3D numerical modeling of high velocity impact of particles in cold spraying by explicit finite element analysis", *Applied Surface Science*, Vol. 255(18), pp. 7878–7892, 2009, doi: 10.1016/j.apsusc.2009.04.135.

[26] S. Rahmati & B. Jodoin, "Physically based finite element modeling method to predict metallic bonding in cold spray", *Journal of Thermal Spray Technology*, Vol. 29, pp. 611–629, 2020, doi: 10.1007/s11666-020-01000-1.

[27] B. Gnanasekaran, G. R. Liu, Y. Fu, G. Wang, W. Niu & T. Lin, "A Smoothed Particle Hydrodynamics (SPH) procedure for simulating cold spray process-A study using particles", *Surface and Coatings Technology*, Vol. 377, 124812, 2019, doi: 10.1016/j.surfcoat.2019.07.036.

[28] A. Manap, K. Ogawa & T. Okabe, "Numerical analysis of interfacial bonding of Al-Si particle and mild steel substrate by cold spray technique using the SPH method", *Journal of Solid Mechanics and Materials Engineering*, Vol. 6(3), pp. 241‑250, 2012, doi: 10.1299/jmmp.6.241.

[29] W. Y. Li, K. Yang, S. Yin & X. P. Guo, "Numerical analysis of cold spray particles impacting behavior by the Eulerian method: a review", *Journal of Thermal Spray Technology*, Vol. 25, pp. 1441–1460, 2016, doi: 10.1007/s11666-016-0443-3.

[30] P. E. Leger, M. Sennour, F. Delloro et al., "Multiscale experimental and numerical approach to the powder particle shape effect on Al-Al_2O_3 coating build-up", *Journal of Thermal Spray Technology*, Vol. 26, pp. 1445‑1460, 2017, doi: 10.1007/s11666-017-0618-6.

[31] W. Y. Li, C. Zhang, C. J. Li, & H. Liao, "Modeling aspects of high velocity impact of particles in cold spraying by explicit finite element analysis", *Journal of Thermal Spray Technology*, Vol. 18, pp. 921–933, 2009, doi: 10.1007/s11666-009-9325-2.

[32] B. Yildirim, S. Muftu, A. Gouldstone, "Modeling of high velocity impact of spherical particles", *Wear*, Vol. 270 (9‑10), pp. 703‑713, 2011, doi: 10.1016/j.wear.2011.02.003.

[33] G. Bae, Y. Xiong, S. Kumar, K. Kang & C. Lee, "General aspects of interface bonding in kinetic sprayed coatings", *Acta Materialia*, Vol. 56(17), pp. 4858‑4868, 2008, doi: 10.1016/j.actamat.2008.06.003.

[34] W. Y. Li, H. Liao, C. J. Li, H. S. Bang & C. Coddet, "Numerical simulation of deformation behavior of Al particles impacting on Al substrate and effect of surface oxide films on interfacial bonding in cold spraying", *Applied Surface Science*, Vol. 253(11), pp. 5084‑5091, 2007, doi: 10.1016/j.apsusc.2006.11.020.

[35] Z. Xiong, L. Mingwan, W. Jianjun, "Research progress on arbitrary Lagrangian-Eulerian description method", *Journal of Computational Mechanics*, Vol. 1, pp. 93‑104, 1997.

[36] W. Feng, Z. Ming, "Numerical analysis of the deposition process of cold spray particles on the surface of cast iron and Q235 steel", *Materials Herald*, Vol. 30(10), pp. 135‑138, 2016.

[37] W. Hequan, Z. Bo, Y. Fuhe, "Research on residual stress detection and simulation of plasma sprayed NiCrAl coating on titanium alloy surface", *Thermal Processing Technology*, Vol. 47(22), pp. 147‑151, 2018.

[38] W.-Y. Li; S. Yin; X.-F. Wang, Numerical investigations of the effect of oblique impact on particle deformation in cold spraying by the SPH method, *Applied Surface Science*, Vol. 256(12), pp. 3725‑3734, 2010, doi: 10.1016/j.apsusc.2010.01.014.

[39] Shuo Yin; Xiao-fang Wang; Bao-peng Xu; Wen-ya Li. (2010), "Examination on the Calculation Method for Modeling the Multi-Particle Impact Process in Cold Spraying", *Journal of Thermal Spray Technology*, Vol. 19(5), pp. 1032‑1041, doi: 10.1007/s11666-010-9489-9.

[40] Dassault Systemes. ABAQUS Analysis User's Manue. 6.11 ed. Simulia. Providence. Chap. 24 (2011).

[41] S. Bagherifard, S. Monti, M. V. Zuccoli, M. Riccio, J. Kondás and M. Guagliano, "Cold spray deposition for additive manufacturing of freeform structural components compared to selective laser melting", *Materials Science and Engineering: A*, Vol. 721, pp. 339‑350, 2018, doi: 10.1016/j.msea.2018.02.094.

[42] M. Hassani-Gangaraj, D. Veysset, V. K. Champagne, K. A. Nelson and C. A. Schuh, "Adiabatic shear instability is not necessary for adhesion in cold spray", *Acta Materialia*, Vol. 158, pp. 430‑439, 2018, doi: 10.1016/j.actamat.2018.07.065.

[43] B. Yildirim, S. Muftu & A. Gouldstone, "Modeling of high velocity impact of spherical particles", *Wear*, Vol. 270 (9‑10), pp. 703‑713, 2011, doi: 10.1016/j.wear.2011.02.003.

[44] D. MacDonald, R. Fernández, F. Delloro and B. Jodoin, "Cold spraying of armstrong process titanium powder for additive manu-facturing", *Journal of thermal spray technology*, Vol. 26, pp. 598‑609, 2017, doi: 10.1007/s11666-016-0489-2.

[45] S. H. Zahiri, D. Fraser, S. Gulizia and M. Jahedi, "Effect of processing conditions on porosity formation in cold gas dynamic spraying of copper", *Journal of thermal spray technology*, Vol. 15, pp. 422–430, 2006, doi: 10.1361/105996306X124437.

[46] S.Weiller, F. Delloro, "A numerical study of pore formation mechanisms in aluminium cold spray coatings", *Additive Manufacturing*, Vol. 60, 103193, 2022, doi: 10.1016/j.addma.2022.103193.

[47] M. Terrone, A. A. Lordejani, J. Kondas and S. Bagherifard, "A numerical approach to design and develop freestanding porous structures through cold spray multi-material deposition", *Surface and Coatings Technology*, Vol. 421, 127423, 2021, doi: 10.1016/j.surfcoat.2021.127423

[48] J. Xie et al., "Simulation of the cold spray particle deposition process", *Journal of Tribology*, Vol. 137(4), 041101, 2015, doi: 10.1115/1.4030257

[49] Y. Wang, J. Adrien & B. Normand, “Porosity characterization of cold sprayed stainless steel coating using three-dimensional X-ray microtomography”, *Coatings*, 8(9), 326, 2018, doi: 10.3390/coatings8090326

[50] X. Song, K. L. Ng, J. M.-K. Chea et al., “Coupled Eulerian-Lagrangian (CEL) simulation of multiple particle impact during Metal Cold Spray process for coating porosity prediction”, *Surface and Coatings Technology*, Vol. 385, 125433, 2020, doi: 10.1016/j.surfcoat.2020.125433

[51] S. Weiller, F. Delloro, P. Lomonaco, M. Jeandin & C. Garion, “A finite elements study on porosity creation mechanisms in cold sprayed coatings”, *Key Engineering Materials*, Vol. 813, pp. 358‑363, 2019, doi: 10.4028/www.scientific.net/kem.813.358.

[52] K. Tan, W. Hu, O. Shorinov & Y. Wang, “Simulating multi-particle deposition based on CEL method: studing the effects of particle and substrate temperature on deposition”, *Aerospace Technic and Technology*, No. 1, pp. 64–75, 2024, doi: 10.32620/aktt.2024.1.06

[53] H. Manafi Farid, A. McDonald & J. D. Hogan, “Impact Deposition Behavior of Al/B4C Cold-Sprayed Composite Coatings: Understanding the Role of Porosity on Particle Retention”, *Materials*, 16(6), 2525, 2023, doi: 10.3390/ma16062525.

[54] W. Xie, A. Alizadeh-Dehkharghani, Q. Chen et al., “Dynamics and extreme plasticity of metallic microparticles in supersonic collisions”, *Scientific reports*, 7(1), 5073, 2017, doi: 10.1038/s41598-017-05104-7

[55] F. Dušek, “Plastic deformation at high strain rates”, *Czech J Phys*., Vol. 20, pp. 776‑789, 1970, doi: 10.1007/BF01726605.

[56] JAHM Software Inc., Material Properties Database. MPDB (2003); V7.01 demo.

[57] E. Lin, Q. Chen, O. C. Ozdemir et al., “Effects of Interface Bonding on the Residual Stresses in Cold-Sprayed Al-6061: A Numerical Investigation”, *Journal of Thermal Spray Technology*, Paper No: itsc2018p0278, pp. 278–285, 2018, doi: 10.31399/asm.cp.itsc2018p0278

Моделювання впливу мультичасткової температури на пористість покриття Al6061 на основі методу зв’язаного Ейлерова-Лагранжа (CEL)

Кунь Тань[1]

[1] *Національний аерокосмічний університет ім. М. Є. Жуковського “Харківський авіаційний інститут”, Харків, Україна*

Анотація. *Холодне розпилення – це технологія твердотільного осадження, яка широко використовується в адитивному виробництві. Температура частинок здебільшого використовується для регулювання пористості покриття. У цій статті використовується скрипт Python для моделювання мультичастинкової моделі; потім мультичастинкова модель вкладається в модель осадження CEL для імітації фактичного процесу мультичастинкового осадження холодним розпиленням; метод CEL має характеристики високої точності та надійності і був обраний в якості методу моделювання для моделі мультичастинкового осадження. Пористість покриття виражається шляхом вивчення величини площі пустот EVF в до-майданчику Ейлера. На поверхні покриття було відібрано кілька груп зразків для розрахунку пористості кожної групи, а середнє значення було прийнято за пористість всього покриття. Чисельні результати показують, що підвищення температури частинок може ефективно зменшити пористість покриття. Середня пористість покриття при температурі частинок 600 K: 5,08 %; 650 K: 4,02 %; 700 K: 3,58 %; після завершення осадження внутрішня частина покриття виглядає ущільненою. Температура підкладки впливає на поєднання покриття та підкладки. Рекомендується, щоб різниця температур між частинками і підкладкою не була занадто великою. Метод CEL імітує процес мультичастинкового осадження холодним розпиленням, що є ефективним методом спостереження і прогнозування пористості покриття, який також недосяжний для методів SPH і ALE.*

Ключові слова: *холодне розпилення, CEL, осадження, температура, мультичастинковість, пористість, підкладка.*